Synthesis of RNA nucleotides in plausible prebiotic conditions from ab initio computer simulations

Andrea Pérez-Villa, Antonino Marco Saitta, Thomas Georgelin, Jean-François Lambert, François Guyot, Marie-Christine Maurel, Fabio Pietrucci

Synthesis of RNA nucleotides in plausible prebiotic conditions from ab initio computer simulations

Andrea Pérez-Villa,[†] A. Marco Saitta,[*,†] Thomas Georgelin,[‡,¶] Jean-François Lambert,[‡] François Guyot,[†] Marie-Christine Maurel,[§] and Fabio Pietrucci[*,†]

†*Sorbonne Université, Muséum National d'Histoire Naturelle, UMR CNRS 7590, IRD, Institut de Minéralogie, de Physique des Matriaux et de Cosmochimie, IMPMC, F-75005 Paris, France*

‡*Sorbonne Université, CNRS UMR 7197, Laboratoire de Réactivité de Surface, LRS, F-75005 Paris, France*

¶*Centre de Biophysique Moléculaire, CNRS UPR 4301, F-45071 Orléans, France*

§*Sorbonne Université, Muséum National d'Histoire Naturelle, CNRS MNHN UMR 7205, Institut de Systématique, Evolution, Biodiversité, ISyEB, F-75005 Paris, France*

E-mail: marco.saitta@sorbonne-universite.fr; fabio.pietrucci@sorbonne-universite.fr

Abstract

Understanding the mechanism of spontaneous formation of ribonucleotides under realistic prebiotic conditions is a key open issue of origins-of-life research. In cells, *de novo* and salvage nucleotide enzymatic synthesis combines 5-phospho-α-D-ribose-1-diphosphate (α-PRPP) and nucleobases. Interestingly, these reactants are also known as prebiotically plausible compounds. Combining ab initio molecular dynamics simulations with recently developed reaction exploration and enhanced sampling methods, we show that nucleobases and α-PRPP should spontaneously combine, under mild hydrothermal conditions, with an exothermic reaction and a facile mechanism, forming both purine and pyrimidine ribonucleotides. Surprisingly, this mechanism is very similar to the biological one, and yields ribonucleotides with the same anomeric carbon chirality as in biological systems. **Mass spectrometry experiments performed on solutions of adenine and PRPP in similar conditions support the formation of AMP.** These results suggest that natural selection might have optimized – through enzymes – a pre-existing ribonucleotide formation mechanism, carrying it forward to modern life forms.

Graphical TOC Entry

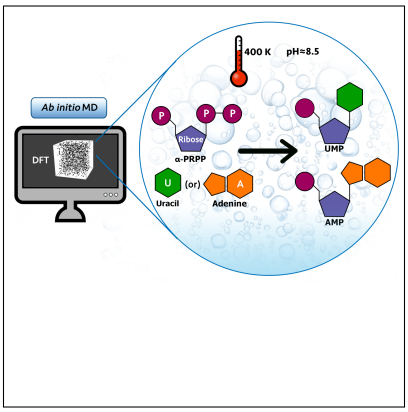

Exploring the synthesis and functionality of nucleic acid molecules is one of the key issues in the origins-of-life research. Since the late 80's, scientists have proposed[1] the possibility of a 'RNA world' as the precursor of current biochemistry, a hypothesis strongly supported by the high versatility of RNA molecules to perform different biochemical processes, such as catalysis, gene regulation, storage of information and self-replication, that are fundamental features involved in the development and propagation of life. A plausible RNA world implies sufficiently successful synthesis of the RNA monomers, namely ribonucleotides (or simply nucleotides), followed by their accumulation, their subsequent polymerization and their further propagation and persistence in the environment of occurrence.[2–4] All these steps are affected by a great number of factors (temperature, presence of catalytic surfaces, pH, ionic strength, and so forth), and their plausibility is mainly determined by the thermodynamics and kinetics of the chemical reactions involved.

In the last decades, many efforts have been made in addressing some of these questions. Nucleotides are composed of three chemical subunits: a ribose in its $\beta-$furanose conformation, a nucleobase (purine or pyrimidine) and a phosphate group at the 5' position of the sugar. One of the most challenging issues has been the synthesis of both purine and pyrimidine nucleotides. Different prebiotic setups have successfully yielded nucleobases,[5–8] sugars and their phosphate derivatives;[9,10] however, the assembly of these subunits to constitute the first nucleotides has presented several obstacles.[2,11–13]

Several strategies to produce nucleotides under prebiotic conditions have been assessed. Among them, the nucleoside phosphorylation has been one of the most widely studied.[14] From previous works, pyrimidine and purine nucleosides were phosphorylated after a treatment with different phosphate minerals,[15] or in phosphate solutions with the addition of phosphorylating agents such as urea,[16] another prebiotically relevant substrate. More recent works by Burcar and collaborators,[17] addressed the phosphorylation of sugars and nucleosides using eutetic solvents such as urea/ammonium formate/water (UAFW) upon heating. In 2009, Powner *et al.*[18] proposed an elegant synthetic pathway that involved the reaction

between prebiotically relevant non-canonical subunits of the nucleotides that led to pyrimidine nucleotides. Along very different synthetic routes, experiments performed by Becker *et al.*[19] in 2016, successfully explored purine nucleoside synthesis following the formamidopyrimidine (FaPy) pathway. A coherent prebiotic picture, encompassing the formation of both purine and pyrimidine nucleotides in similar conditions has been one of the largest current challenges in the origin of life field. In this regard, two recent works by Stairs *et al.*[20] and Kim and Benner[21] addressed the synthesis of both types of ribonucleotides along different chemical routes.

In current living organisms and metabolic systems, the *de novo* and salvage synthesis of purine and pyrimidine nucleotides implies a direct reaction between the nucleobase and a molecule of PRPP, a biological metabolite highly activated in C1' due to the presence of the pyrophosphate group. This reaction is mediated by the enzymatic catalysis of phosphoribosyltransferases specific of each nucleobase.[22,23] Primitive biochemical systems have evolved to modern ones improving their performance and selectivity: from this point of view, an interesting question is to understand whether features observed in contemporary enzymatic reactions have been conserved from prebiotic non-enzymatic pathways (chemiomimesis).[24,25] In particular, one can wonder whether PRPP also played a crucial role as precursor of nucleotides in the context of a RNA world.[26] In this work we examined this hypothesis (Fig. 1), which is supported by the possibility to generate PRPP as a ribose phosphorylation product,[27,28] and by its plausibility to operate as a reactant toward nucleotides[28] and nucleotide mimics (ribose-pyrazole derivatives).[29] Furthermore, PRPP takes also part in histidine and purine biosynthesis and might have played a role in their RNA world-counterpart.[30] **Moreover, a previous *ab initio* study reported by Sponer et al[31] addressed the formation of RNA nucleosides starting from RPP (rybosyl-pyrophosphate), a molecule very similar to PRPP, by gas-phase quantum chemistry calculations showing the role of pyrophosphate in the C1' as an optimal leaving group during the glycosylation reaction with the nucleobase.**

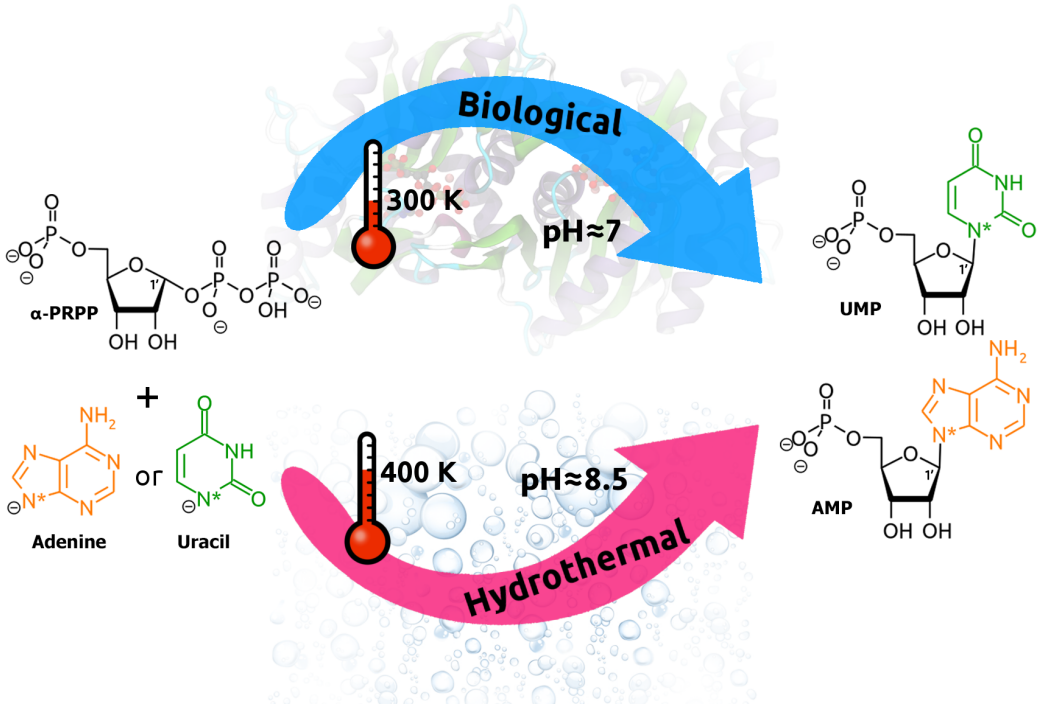

Figure 1: **Pictorial representation of** nucleotide formation from PRPP and purine/pyrimidine bases: current biological pathway versus putative prebiotic hydrothermal conditions suggested from the present work. Current living forms exploit the enzymatic catalysis of phosphoribosyltransferases.

We considered mild hydrothermal conditions, that are compatible with different proposed origin-of-life scenarios, including hot surface lagoons/lakes and submarine or continental hydrothermal systems.[32] We underline that we deliberately choose the simplest possible setting that allows to prove the general thermodynamic viability of the ribonucleotide synthesis reactions.

To address this crucial question, a combination of quantum-based computer simulations and novel advanced enhanced sampling and chemical exploration methods was carried out. *Ab initio* computer simulations in prebiotic chemistry under aqueous solutions[33–36] are very challenging due to the large system size (several hundred atoms), the bulk conditions that have to be taken into account (such as temperature, pH, ionic strength, and so forth), and especially because of the long time scale of chemical reactions. To overcome the latter obstacle, we exploited a new general approach able to simulate complex reaction mechanisms

in solution, combining enhanced sampling techniques (such as metadynamics and umbrella sampling[37–40]) with topological coordinates capable of tracking changes in the chemical bond network.[41] This recent approach proved effective in the simulation of chemical reactions fully accounting for the role of temperature and solvent, including the decomposition[42] and dimerization[43] of amino acids and the synthesis of erythrose,[44] among others. In the present work, we significantly step-up the complexity of the system by tackling the challenging ab initio simulation of nucleotide synthetic pathways.

We have assessed the formation of uridine monophosphate (UMP) and adenosine monophosphate (AMP) starting from α-PRPP and uracil or adenine, respectively, simulating easily-accessible hydrothermal/hot lagoon conditions (T = 400 K, neutral pH), in pure water without any catalyst. Our protocol employs a preliminary exploration of the reaction pathways with metadynamics, followed by the collection of extended statistics exploiting committor analysis and umbrella sampling (see Materials and Methods section).

We have discovered a simple pathway for the association of PRPP with the nucleobase, where the nitrogen forming the glycosidic bond is initially deprotonated. In both purine and pyrimidine cases, the reaction follows a nucleophile substitution S_N2 mechanism, with an inversion of chirality of the anomeric carbon. In Fig. 2 is reported the free energy profile of the reaction, while Fig. 3 displays the detailed atomic configuration of representative reactant, transition state and products structures. The transition state exhibits a trigonal bipyramidal geometry, where C1' becomes planar with O and N nucleophiles from pyrophosphate and nucleobase molecules at a distance of 2.08 and 2.40 Å, respectively, for the pyrimidine, and 2.12 and 2.84 Å for the purine. The reaction connecting the deprotonated nucleobase with the nucleotide follows Hammond's postulate, *i.e.*, the transition state is more similar to the reactants than to the products, since the forward barrier is smaller than the reverse one.[45] When comparing the biological synthesis mediated by enzymes with the simulated prebiotic reactions, it is observed that some mechanistic details are featured in both cases: for instance the nucleobase has to be deprotonated so it can perform the nucleophilic attack on the

C1';[46,47] moreover around the transition state region, C1' adopts a planar geometry during the nucleophilic attack by the base, necessary to undergo the inversion of the chirality when forming the β-nucleotide (see also Figure S1, depicting electron localization function (ELF) analysis[48]). **We note that the solvent plays an important role in this reaction, where reactants, products and transition states are all in ionic forms. Moreover, proton transfers between phosphate oxygens, mediated by solvent molecules, are frequently observed in our simulations (see also movies in SI).** Overall, our results suggest that the reaction should be favored by a mildly basic pH: above 8, based on the pKa $\approx$ **7.3 and 8.5 of U and A, respectively extrapolated at 400 K[49,50] (see SI for further details)**, and below 9, to avoid degradation of PRPP.[27] For similar reasons, under the above conditions an excess of nucleobase should increase the probability of reactive collisions with the PRPP molecule.

Following glycosylation, nucleobases could in principle bind to ribose through other sites than N9 for purines and N1 for pyrimidines. We note, however, that in deprotonated uracil the most stable resonance structure features the negative charge on N1,[51] indicating that the glycosidic bond is more likely to be formed on that site. In the case of adenine, a specific regioselectivity study should be performed, to distinguish the different possible sites for the formation of the glycosidic bond.

In order to assess if our theoretical predictions are experimentally valid, we have carried out a mass spectrometric analysis of a PRPP + A solution activated at 120^{o}C in a closed reactor at pH=8.5 (Fig. 5). We first checked by ^{31}P NMR that the initial reagents did not contain AMP (see Fig. S4 in SI). In the PRPP+A solution, in addition to the starting molecules, we observed the characteristic signal of AMP at 345.9 amu, and confirmed this assignment by studying its fragmentation in the MS/MS mode. Thus, the formation of AMP is effectively observed; however, the yield is rather low because this reaction is in competition with PRPP degradation yielding products such as ribose phosphates and cyclic

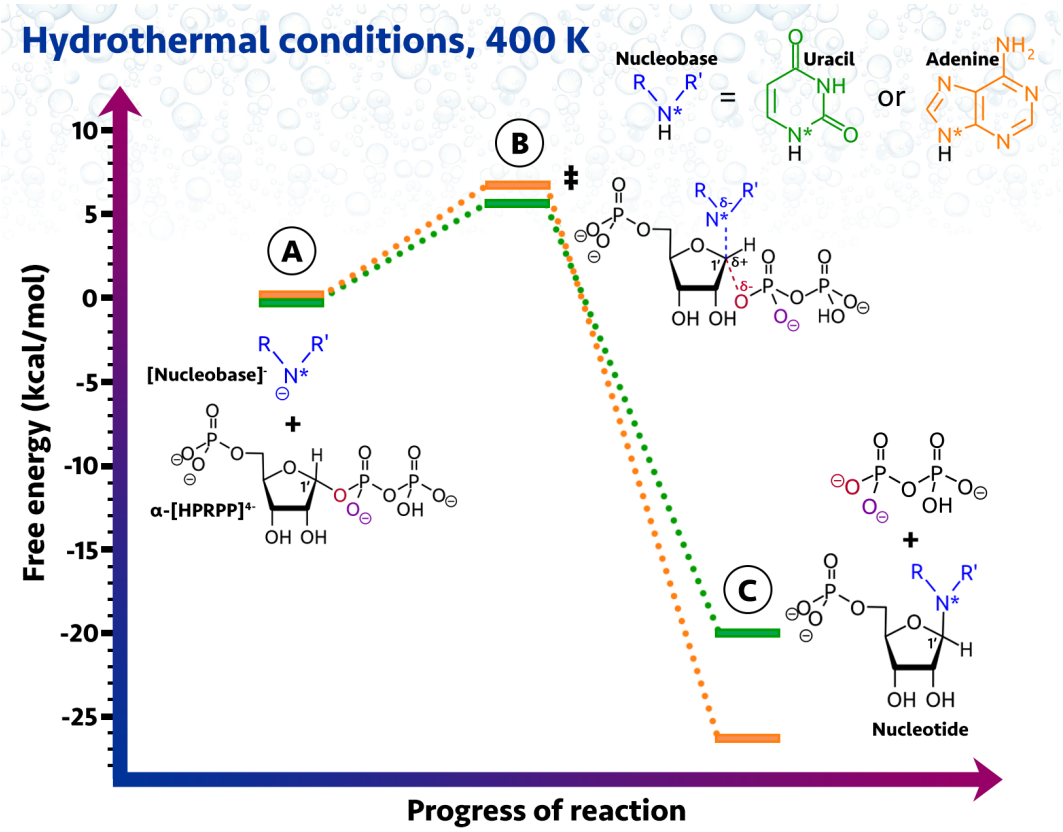

Figure 2: Relative free-energy values for reactants (**A**, arbitrarily set to zero), transition states (**B**), and products for the nucleotide synthesis (**C**). Free-energy levels for uracil (pyrimidine) and adenine (purine) pathways are depicted in green and orange respectively. "**N***" represents the nitrogen from the nucleobase participating in the glycosidic bond. **State A results from a proton transfer from the nucleobase to PRPP, with a free energy cost estimated as 3.3 and 1.2 kcal/mol for uracil and adenine, respectively (see Supporting Information).**

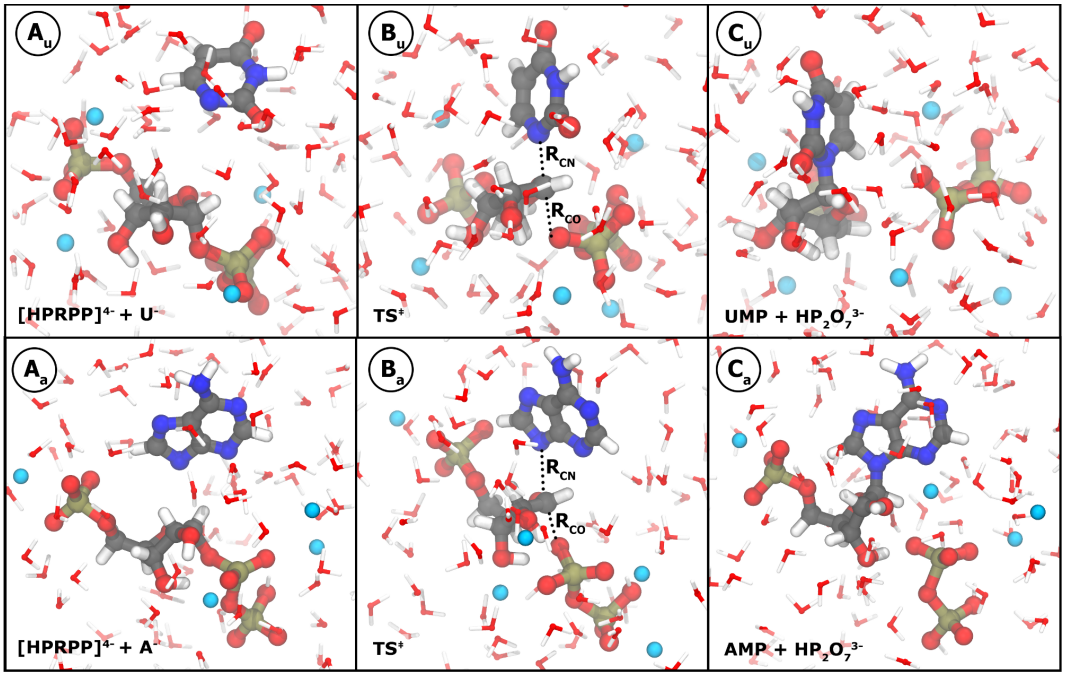

Figure 3: Representative structures of reactants ($\mathbf{A}_\mathrm{u}$ and $\mathbf{A}_\mathrm{a}$), transition states ($\mathbf{B}_\mathrm{u}$ and $\mathbf{B}_\mathrm{a}$), and products ($\mathbf{C}_\mathrm{u}$ and $\mathbf{C}_\mathrm{a}$) during the nucleotide formation from PRPP and uracil or adenine, respectively. The transition states are identified by committor analysis and display the typical geometry of S_N2 mechanisms.

phosphates, following hydrolysis of the C-O-P and P-O-P bonds. Further work is needed to understand the competition between hydrolytic degradation and nucleotide formation and determine what experimental conditions favor the latter pathway. For instance, carrying out the reaction in the presence of mineral surfaces might be helpful since they have been shown to favor the synthesis and stability of PRPP,[28] especially if the scenario implies wetting-drying cycles.[52,53]

In conclusion, we present hereby two main discoveries. First, we identify a new synthetic route spontaneously leading to *both* purine and pyrimidine ribonucleotides, starting from precursors of *both* prebiotic and biological relevance. This route is compatible with several hydrothermal environments, from submarine vents to surface lagoons and lakes, most likely present in the early Earth as well as on other planets. In this context, mineral surfaces could have played an important role in the synthesis and stabilization of PRPP, as well as in improving nucleotide condensation yields by reducing water activity.[28] Second, we demon-

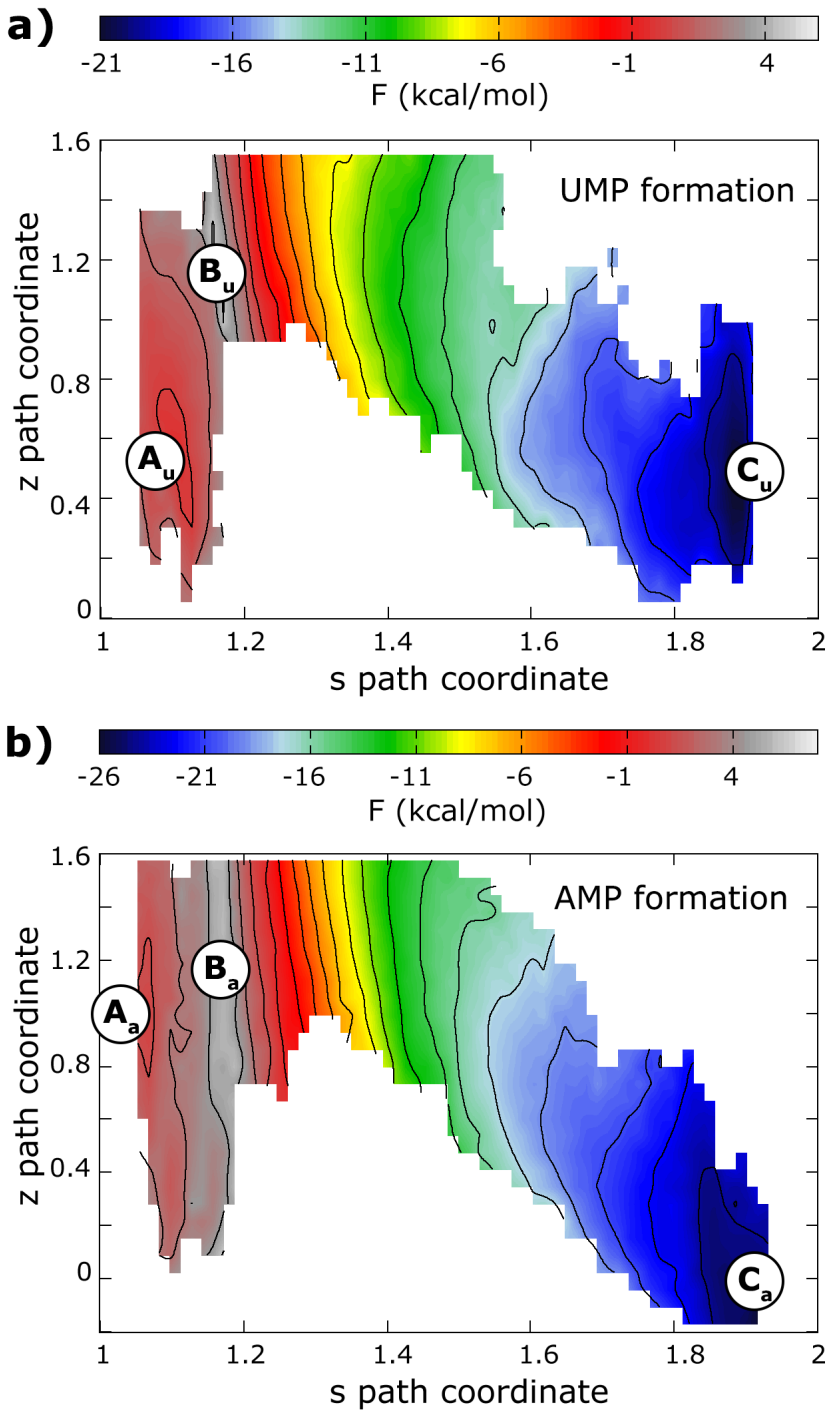

Figure 4: Free energy as a function of the path collective variables s and z for nucleotide formation. Panel **a)** and **b)** are associated to UMP and AMP synthesis respectively. Region $\mathbf{A}_{\mathrm{u}}/\mathbf{A}_{\mathrm{a}}$ correspond to deprotonated nucleobase and PRPP, while $\mathbf{B}_{\mathrm{u}}/\mathbf{B}_{\mathrm{a}}$ and $\mathbf{C}_{\mathrm{u}}/\mathbf{C}_{\mathrm{a}}$ indicate the transition state and nucleotide (UMP and AMP) regions respectively. Levels in the contour map correspond to increments of 1.7 kcal/mol.

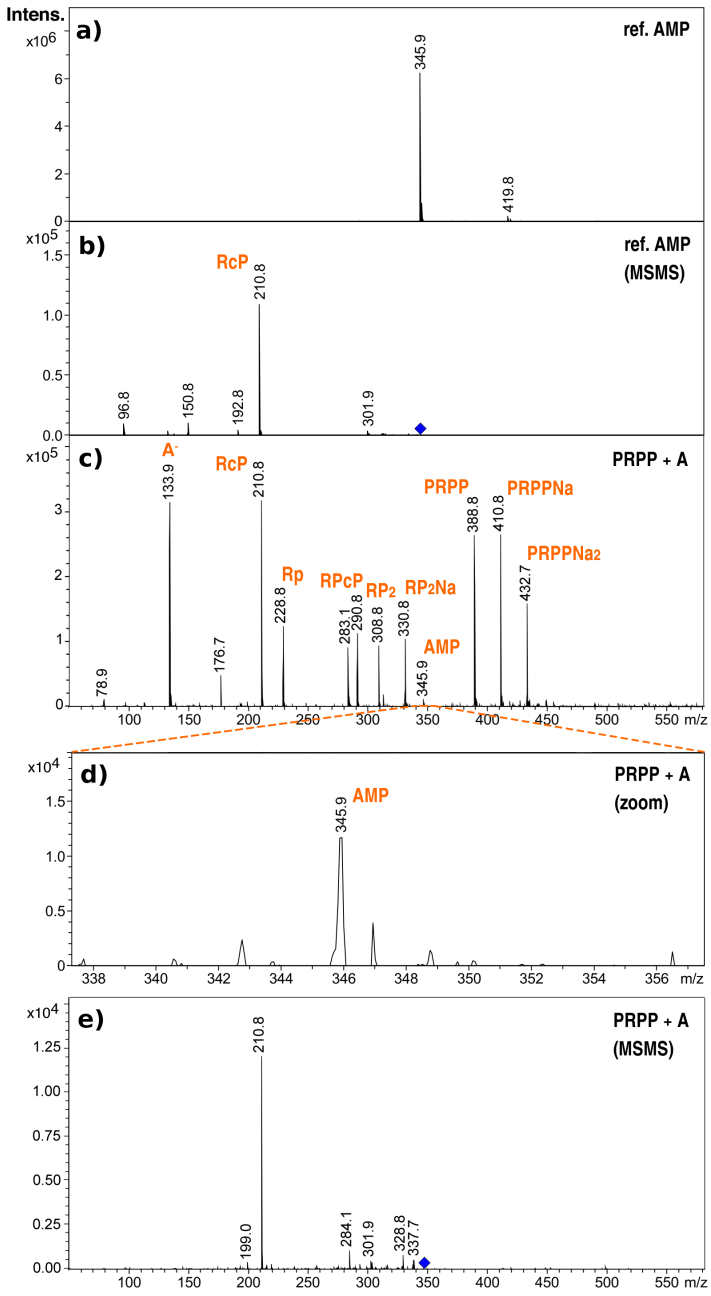

Figure 5: **Mass spectrometry (ESI-IT-MS –negative mode) of (a) AMP reference solution, with the peak at 345.9 amu corresponding to $(AMP–1H)^-$, (b) fragmentation of peak at 345.9 amu in AMP reference, (c) complete spectrum for PRPP + adenine solution activated at 120 ^oC, (d) same spectrum zoomed in the AMP region (337-358 amu), and (e) fragmentation of the peak at 345.9 amu from the PRPP + adenine sample. Peak labeling: A, adenine; RP, ribose phosphate; RcP, ribose cyclic phosphate; RP_2, ribose diphosphate; RPcP, ribose-phosphate-cyclic phosphate (See SI for further details)**

strate, with atomic-level precision, that this spontaneous prebiotic synthetic pathway is very similar to the biological one, to the point of sharing the same precursors, the same steps, and the same chirality-inverting character (Fig. 1). This correspondence is highly suggestive of an evolution process towards complex life forms conserving the basic features of prebiotic ribonucleotide synthesis. Our work demonstrates also the possibility of simulating chemical reactions in systems as large as RNA nucleotides in an explicit bulk solution environment, and of reconstructing the corresponding free energy landscapes, all at the *ab initio* level. **Finally, we present mass-spectrometric experimental evidence that supports the proposed nucleotide formation mechanism.** Building upon all these findings, further studies will be able to experimentally test the new mechanism **on a series of nucleotides in a range of environments**, and to assess under which precise conditions reactions can proceed up the ladder of complexity, starting from the oligomerization of nucleotides, until the possible inception of a fully-functional RNA world.

Materials and Methods

Born-Oppenheimer Molecular Dynamics (BOMD). *Ab initio* calculations were based on the Density Functional Theory with the exchange-correlation Perdew-Burke-Ernzerhof functional,[54] including Grimme's dispersion corrections[55,56] and the Martins-Troullier pseudopotentials[57] for C, N, O, Na, P and H atoms **(with a cutoff of 70 Ry)**, as implemented in the code CPMD 4.1.[58] BOMD simulations were performed in the canonical ensemble (NVT) at a temperature of 400 K, with a time step of ∼0.48 fs, in a periodically repeated cubic box of approximately 4.296 and 4.292 nm^3, and a density of 0.9888 and 0.9984 g/cm^3 for UMP and AMP respectively. Temperature was controlled by the Nosé-Hoover thermostat[59,60] with a chain length of four and with a frequency of 3000 cm^{-1}. The electronic convergence criterion has been set to 10^{-5} a.u. based on benchmark NVE simulations. The simulation boxes comprise a PRPP molecule with charge 5- and a uracil/adenine molecule (reactants) or a

nucleoside monophosphate molecule (UMP or AMP) and a pyrophosphate ion in its $HP_2O_7^{3-}$ form (products), with additional sodium counterions and 108 explicit water molecules, for a total of 371 atoms in the pyrimidine setup and 374 for the purine.

Enhanced Sampling. BOMD simulations were coupled with enhanced sampling techniques.[40] In the first place we performed metadynamics simulations,[37,38] employing as set of reaction coordinates the path collective variables (pathCV) s and z by Branduardi et al.[61] In general, s indicates the progress along a putative pathway composed by a discrete sequence of atomic configurations, while z represents the distance from the putative pathway (complete definitions are provided in Supporting Text reported in SI). In this work, we employed only two reference configurations, corresponding to reactants and products, in this way avoiding to bias the observed reaction mechanisms with hypotheses on the path. In addition, we used the topological metric of Ref.,[41] accurately tracking changes in the chemical bond network passing from reactants, through intermediates, until the products, particularly suited to chemical reactions in solution.[42–44] This metric comparing structure $R(t)$ with reference structure R_k is defined as $D(R, R_k) = \sum_{IS} \left[C_{IS} - C_{IS}^k\right]^2$, where coordination numbers of a specific atom I with the atoms of species S appear (see also Tables S1-S4 in SI).

In the second stage, we carried out a committor analysis[62] to identify the transition state of each reaction and to get more insights about its mechanism. We extracted a set of about 10 atomic configurations from reactive metadynamics trajectories, and we performed up to 20 independent unbiased BOMD trajectories of 0.5 ps starting from each configuration, verifying whether they fell into reactants or products basins. A transition state configuration is identified as committed to both basins with a probability of 50±10%.

In the final stage, a series of umbrella sampling[39] simulations were performed, systematically restraining the s coordinate at different locations along the reaction pathway obtained by committor analysis using an harmonic potential (all details are reported in SI, Table S5). The trajectory length of each window was 10 ps, for a total simulation time of 250 and 220 ps for the pyrimidine and purine cases, respectively. The weighted histogram analysis

method[63] finally yielded the free energy profile of the reactions, with an estimated error bar of 1 kcal/mol for the pyrimidine case and of 1.5 kcal/mol for the purine case. All enhanced sampling simulations employed a modified version of the plugin Plumed 1.3.[64]

Mass Spectrometry. **We used pure PRPP and adenine purchased from Sigma Aldrich. Fig. S4 in SI demonstrates the lack of nucleotide contaminants in the initial solution as verified with ^{31}P NMR spectroscopy. A mixture of PRPP and adenine was prepared by dissolving 12.5 mg of PRPP (0.05 mol/L) in 500 μL of milliQ water and adding 13.5 mg of adenine (0.2 mol/L). The pH was adjusted to 8.5 by controlled addition of NaOH. This mixture was heated to 120 ^{o}C during 15 minutes in a closed glass vial and filtered on 2 μm filter paper. It was then diluted to the micromolar range in a solution of 50% acetonitrile, 49.8% water and analyzed by direct infusion in a HCT Ultra PTM Discovery mass spectrometer from Bruker Daltonics (Germany) equipped with an electrospray ion source. The nebulizer gas pressure was 11 psi and the spray voltage was ~3.5 kV. The drying gas flow was 5 L/min and the temperature was 300 ^{o}C. Spectra were acquired in negative ion MS mode over a 50–2000 m/z range until the ion charge control target had reached 90000.**

Acknowledgement

This work was supported by French state funds managed by the ANR within the Investissements d'Avenir programme under reference ANR-11-IDEX-0004-02, within the framework of the cluster of excellence MATériaux Interfaces Surfaces Environnement (MATISSE) led by Sorbonne Universités. We acknowledge calculations performed on the *Ada* cluster at IDRIS, (Orsay, France) under GENCI allocations 2015-091387 and 2016-091387; and *Curie* Supercomputer at TGCC under GENCI allocations t201609s042 and A0010910143.

Supporting Information Available

Complementary computational details of enhanced sampling simulations. Graphical representation of Electron Localization Function (ELF) analysis performed for reactants, TS and products. This material is available free of charge via the Internet at `http://pubs.acs.org/`.

References

(1) Gilbert, W. Origin of life: The RNA world. *Nature* **1986**, *319*, 618–618.

(2) Lazcano, A.; Miller, S. L. The Origin and Early Evolution of Life: Prebiotic Chemistry, the Pre-RNA World, and Time. *Cell* **1996**, *85*, 793–798.

(3) Benner, S. A.; Kim, H.-J.; Yang, Z. Setting the Stage: The History, Chemistry, and Geobiology behind RNA. *Cold Spring Harb. Perspect. Biol.* **2012**, *4*, a003541.

(4) Sutherland, J. D. The Origin of Life – Out of the Blue. *Angew. Chem. Int. Ed.* **2016**, *55*, 104–121.

(5) Oró, J. Synthesis of adenine from ammonium cyanide. *Biochem. Biophys. Res. Commun.* **1960**, *2*, 407 – 412.

(6) Sanchez, R. A.; Ferris, J. P.; Orgel, L. E. Studies in prebiotic synthesis. *J. Mol. Biol.* **1968**, *38*, 121 – 128.

(7) Robertson, M. P.; Miller, S. L. An efficient prebiotic synthesis of cytosine and uracil. *Nature* **1995**, *375*, 772–774.

(8) Hudson, J. S.; Eberle, J. F.; Vachhani, R. H.; Rogers, L. C.; Wade, J. H.; Krishnamurthy, R.; Springsteen, G. A Unified Mechanism for Abiotic Adenine and Purine Synthesis in Formamide. *Angew. Chem. Int. Ed.* **2012**, *51*, 5134–5137.

(9) Pitsch, S.; Eschenmoser, A.; Gedulin, B.; Hui, S.; Arrhenius, G. Mineral induced formation of sugar phosphates. *Orig. Life. Evol. Biosph.* **1995**, *25*, 297–334.

(10) Gibard, C.; Bhowmik, S.; Karki, M.; Kim, E.-K.; Krishnamurthy, R. Phosphorylation, oligomerization and self-assembly in water under potential prebiotic conditions. *Nat Chem* **2017**, *10*, 212–217.

(11) Cafferty, B. J.; Hud, N. V. Abiotic synthesis of RNA in water: a common goal of prebiotic chemistry and bottom-up synthetic biology. *Curr. Opin. Chem. Biol.* **2014**, *22*, 146–157.

(12) Krishnamurthy, R. On the Emergence of RNA. *Isr. J. Chem.* **2015**, *55*, 837–850.

(13) Islam, S.,; Powner, M. W., Prebiotic Systems Chemistry: Complexity Overcoming Clutter. *Chem* **2018**, *2*, 470–501.

(14) Gull, M. Prebiotic Phosphorylation Reactions on the Early Earth. *Challenges* **2014**, *5*, 193–212.

(15) Schwartz, A. W.; van der Veen, M.; Bisseling, T.; Chittenden, G. J. F. Prebiotic nucleotide synthesis-demonstration of a geologically plausible pathway. *Orig. Life Evol. Biospheres* **1975**, *6*, 163–168.

(16) Reimann, R.; Zubay, G. Nucleoside Phosphorylation: A Feasible Step in the Prebiotic Pathway to RNA. *Orig. Life Evol. Biospheres* **1999**, *29*, 229–247.

(17) Burcar, B.; Pasek, M.; Gull, M.; Cafferty, B. J.; Velasco, F.; Hud, N. V.; MenorSalvn, C. Darwin's Warm Little Pond: A OnePot Reaction for Prebiotic Phosphorylation and the Mobilization of Phosphate from Minerals in a UreaBased Solvent. *Angew. Chem.* **2016**, *128*, 13443–13447.

(18) Powner, M. W.; Gerland, B.; Sutherland, J. D. Synthesis of activated pyrimidine ribonucleotides in prebiotically plausible conditions. *Nature* **2009**, *459*, 239–242.

(19) Becker, S.; Thoma, I.; Deutsch, A.; Gehrke, T.; Mayer, P.; Zipse, H.; Carell, T. A high-yielding, strictly regioselective prebiotic purine nucleoside formation pathway. *Science* **2016**, *352*, 833–836.

(20) Stairs, S.; Nikmal, A.; Bucar, D.-K.; Zheng, S.-L.; Szostak, J. W.; Powner, M. W. Divergent prebiotic synthesis of pyrimidine and 8-oxo-purine ribonucleotides. *Nat. Commun.* **2017**, *8*, 15270.

(21) Kim, H.-J.; Benner, S. A. Prebiotic stereoselective synthesis of purine and noncanonical pyrimidine nucleotide from nucleobases and phosphorylated carbohydrates. *Proc. Natl. Acad. Sci. U.S.A.* **2017**, *114*, 11315–11320.

(22) Zrenner, R.; Stitt, M.; Sonnewald, U.; Boldt, R. Pyrimidine and Purine Biosynthesis and Degradation in Plants. *Annu. Rev. Plant Biol.* **2006**, *57*, 805–836.

(23) Nyhan, W. L. *Nucleotide Synthesis via Salvage Pathway. eLS.*; John Wiley & Sons, Ltd, John Wiley & Sons, 2001.

(24) Eschenmoser, A.; Loewenthal, E. Chemistry of potentially prebiological natural products. *Chem. Soc. Rev.* **1992**, *21*, 1–16.

(25) Saladino, R.; Crestini, C.; Ciciriello, F.; Pino, S.; Costanzo, G.; Di Mauro, E. From formamide to RNA: the roles of formamide and water in the evolution of chemical information. *Res. Microbiol.* **2009**, *160*, 441–448.

(26) Kawamura, K.; Maurel, M.-C. Walking over 4 Gya: Chemical Evolution from Photochemistry to Mineral and Organic Chemistries Leading to an RNA World. *Orig. Life. Evol. Biosph.* **2017**, *47*, 281–296.

(27) Dennis, A. L.; Puskas, M.; Stasaitis, S.; Sandwick, R. K. The formation of a 15 phosphodiester linkage in the spontaneous breakdown of 5-phosphoribosyl-α-1-pyrophosphate. *J. Inorg. Biochem.* **2000**, *81*, 73 – 80.

(28) Akouche, M.; Jaber, M.; Maurel, M.-C.; Lambert, J.-F.; Georgelin, T. Phosphoribosyl Pyrophosphate: A Molecular Vestige of the Origin of Life on Minerals. *Angew. Chem.* **2017**, *129*, 8028–8031.

(29) Gopinath, P.; Ramalingam, V.; Breslow, R. Magnesium pyrophosphates in enzyme mimics of nucleotide synthases and kinases and in their prebiotic chemistry. *Proc. Natl. Acad. Sci. U.S.A.* **2015**, *112*, 12011–12014.

(30) Vázquez-Salazar, A.; Becerra, A.; Lazcano, A. Evolutionary convergence in the biosyntheses of the imidazole moieties of histidine and purines. *PLoS ONE* **2018**, *13*, e0196349.

(31) Šponer, J. E.; Šponer, J.; Fuentes-Cabrera, M. Prebiotic Routes to Nucleosides: A Quantum Chemical Insight into the Energetics of the Multistep Reaction Pathways. *Chem. Eur. J.* **2011**, *17*, 847–854.

(32) W. Martin,; J. Baross,; D. Kelley,; M. J. Russell, Hydrothermal vents and the origin of life. *Nat. Rev. Micro* **2008**, *6*, 805814.

(33) Schreiner, E.; Nair, N. N.; Wittekindt, C.; Marx, D. Peptide synthesis in aqueous environments: the role of extreme conditions and pyrite mineral surfaces on formation and hydrolysis of peptides. *J Am. Chem. Soc.* **2011**, *133*, 8216–8226.

(34) Glaves, R.; Mathias, G.; Marx, D. Mechanistic insights into the hydrolysis of a nucleoside triphosphate model in neutral and acidic solution. *J Am. Chem. Soc.* **2012**, *134*, 6995–7000.

(35) Saitta, A. M.; Saija, F. Miller experiments in atomistic computer simulations. *Proc. Natl. Acad. Sci. U.S.A.* **2014**, *111*, 13768–13773.

(36) Šponer, J. E.; Szabla, R.; Góra, R. W.; Saitta, A. M.; Pietrucci, F.; Saija, F.; Di Mauro, E.; Saladino, R.; Ferus, M.; Civiš, S. et al. Prebiotic synthesis of nucleic

acids and their building blocks at the atomic level–merging models and mechanisms from advanced computations and experiments. *Phys. Chem. Chem. Phys.* **2016**, *18*, 20047–20066.

(37) Laio, A.; Parrinello, M. Escaping free-energy minima. *Proc. Natl. Acad. Sci. U.S.A.* **2002**, *99*, 12562–12566.

(38) Laio, A.; Gervasio, F. L. Metadynamics: a method to simulate rare events and reconstruct the free energy in biophysics, chemistry and material science. *Rep. Prog. Phys.* **2008**, *71*, 126601.

(39) Torrie, G.; Valleau, J. Nonphysical sampling distributions in Monte Carlo free-energy estimation: Umbrella sampling. *J. Comput. Phys.* **1977**, *23*, 187 – 199.

(40) Pietrucci, F. Strategies for the exploration of free energy landscapes: unity in diversity and challenges ahead. *Rev. Phys.* **2017**, *2*, 32–45.

(41) Pietrucci, F.; Saitta, A. M. Formamide reaction network in gas phase and solution via a unified theoretical approach: Toward a reconciliation of different prebiotic scenarios. *Proc. Natl. Acad. Sci. U.S.A.* **2015**, *112*, 15030–15035.

(42) Pietrucci, F.; Aponte, J. C.; Starr, R. D.; Pérez-Villa, A.; Elsila, J. E.; Dworkin, J. P.; Saitta, A. M. Hydrothermal Decomposition of Amino Acids and Origins of Prebiotic Meteoritic Organic Compounds. *ACS Earth Space Chem.* **2018**, *doi: 10.1021/acsearthspacechem.8b00025*.

(43) Kroonblawd, M. P.; Pietrucci, F.; Saitta, A. M.; Goldman, N. Generating Converged Accurate Free Energy Surfaces for Chemical Reactions with a Force-Matched Semiempirical Model. *J. Chem. Theory Comput.* **2018**, *14*, 2207–2218.

(44) Cassone, G.; Sponer, J.; Sponer, J. E.; Pietrucci, F.; Saitta, A. M.; Saija, F. Synthe-

sis of (d)-erythrose from glycolaldehyde aqueous solutions under electric field. *Chem. Commun.* **2018**, *54*, 3211–3214.

(45) Hammond, G. S. A Correlation of Reaction Rates. *J. Am. Chem. Soc.* **1955**, *77*, 334–338.

(46) Grubmeyer, C.; Hansen, M. R.; Fedorov, A. A.; Almo, S. C. Structure of Salmonella typhimurium OMP Synthase in a Complete Substrate Complex. *Biochem.* **2012**, *51*, 4397–4405.

(47) Shi, W.; Sarver, A. E.; Wang, C. C.; Tanaka, K. S. E.; Almo, S. C.; Schramm, V. L. Closed Site Complexes of Adenine Phosphoribosyltransferase from Giardia lamblia Reveal a Mechanism of Ribosyl Migration. *J. Biol. Chem.* **2002**, 39981–39988.

(48) Savin, A.; Nesper, R.; Wengert, S.; Fässler, T. F. ELF: The electron localization function. *Angew. Chem. Int. Ed.* **1997**, *36*, 1808–1832.

(49) Camargo, A. P. M.; Baumgartel, H.; Donner, C. Coadsorption of the DNA bases thymine and adenine at the Au(111) electrode. *Phys. Chem. Chem. Phys.* **2003**, *5*, 1657–1664.

(50) Ganguly, S.; Kundu, K. K. Protonation/deprotonation energetics of uracil, thymine, and cytosine in water from e.m.f./spectrophotometric measurements. *Can. J. Chem.* **1994**, *72*, 1120–1126.

(51) Cole, C. A.; Wang, Z.-C.; Snow, T. P.; Bierbaum, V. M. Anionic derivatives of uracil: fragmentation and reactivity. *Phys. Chem. Chem. Phys.* **2014**, *16*, 17835–17844.

(52) Da Silva, L.; Maurel, M.-C.; Deamer, D. Salt-Promoted Synthesis of RNA-like Molecules in Simulated Hydrothermal Conditions. *J. Mol. Evol.* **2015**, *80*, 86–97.

(53) S. Becker,; C. Schneider,; H. Okamura,; A. Crisp,; T. Amatov,; M. Dejmek,; T. Carell,

Wet-dry cycles enable the parallel origin of canonical and non-canonical nucleosides by continuous synthesis. *Nat. Commun.* **2018**, *9*, 163.

(54) Perdew, J. P.; Burke, K.; Ernzerhof, M. Generalized Gradient Approximation Made Simple. *Phys. Rev. Lett.* **1996**, *77*, 3865–3868.

(55) Grimme, S. Semiempirical GGA-type density functional constructed with a long-range dispersion correction. *J. Comput. Chem.* **2006**, *27*, 1787–1799.

(56) Barone, V.; Casarin, M.; Forrer, D.; Pavone, M.; Sambi, M.; Vittadini, A. Role and effective treatment of dispersive forces in materials: Polyethylene and graphite crystals as test cases. *J. Comput. Chem.* **2009**, *30*, 934–939.

(57) Troullier, N.; Martins, J. L. Efficient pseudopotentials for plane-wave calculations. *Phys. Rev. B* **1991**, *43*, 1993–2006.

(58) CPMD Copyright IBM Corp. and by Max Planck Institute Stuttgart. 2000-2017; `http://www.cpmd.org/`.

(59) Nosé, S. A unified formulation of the constant temperature molecular dynamics methods. *J. Chem. Phys.* **1984**, *81*, 511–519.

(60) Hoover, W. G. Canonical dynamics: Equilibrium phase-space distributions. *Phys. Rev. A* **1985**, *31*, 1695–1697.

(61) Branduardi, D.; Gervasio, F. L.; Parrinello, M. From A to B in free energy space. *J. Chem. Phys.* **2007**, *126*, 054103.

(62) Bolhuis, P. G.; Chandler, D.; Dellago, C.; Geissler, P. L. TRANSITION PATH SAMPLING: Throwing Ropes Over Rough Mountain Passes, in the Dark. *Annu. Rev. Phys. Chem.* **2002**, *53*, 291–318.

(63) Kumar, S.; Rosenberg, J. M.; Bouzida, D.; Swendsen, R. H.; Kollman, P. A. The weighted histogram analysis method for free-energy calculations on biomolecules. I. The method. *J. Comput. Chem.* **1992**, *13*, 1011–1021.

(64) Bonomi, M.; Branduardi, D.; Bussi, G.; Camilloni, C.; Provasi, D.; Raiteri, P.; Donadio, D.; Marinelli, F.; Pietrucci, F.; Broglia, R. A. et al. PLUMED: A portable plugin for free-energy calculations with molecular dynamics. *Comput. Phys. Commun.* **2009**, *180*, 1961–1972.